



LAWRENCE  
LIVERMORE  
NATIONAL  
LABORATORY

# Physical Characterization of RX-55-AE-5 A formulation of 97.5 % 2, 6-diamino-3, 5-dinitropyrazine-1-oxide (LLM 105) and 2.5 % Viton A

R. K. Weese, A. K. Burnham, H. C. Turner, T.  
Tran

June 10, 2005

JOWOG 9  
Reading, United Kingdom  
June 22, 2005 through June 24, 2005

## **Disclaimer**

---

This document was prepared as an account of work sponsored by an agency of the United States Government. Neither the United States Government nor the University of California nor any of their employees, makes any warranty, express or implied, or assumes any legal liability or responsibility for the accuracy, completeness, or usefulness of any information, apparatus, product, or process disclosed, or represents that its use would not infringe privately owned rights. Reference herein to any specific commercial product, process, or service by trade name, trademark, manufacturer, or otherwise, does not necessarily constitute or imply its endorsement, recommendation, or favoring by the United States Government or the University of California. The views and opinions of authors expressed herein do not necessarily state or reflect those of the United States Government or the University of California, and shall not be used for advertising or product endorsement purposes.

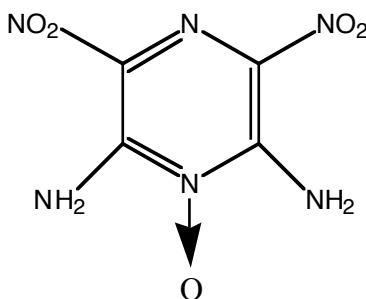
**Physical characterization of RX-55-AE-5  
A formulation of 97.5 % 2,6-diamino-3,5-dinitropyrazine-1-oxide (LLM-105) and  
2.5% Viton A**

Randall K. Weese\*, Alan K. Burnham, Heidi C. Turner and Tri D. Tran  
Energetic Materials Center, Chemistry and Materials Science Directorate,  
Lawrence Livermore National Laboratory  
7000 East Avenue Livermore, L-282, California, 94550, USA

E-mail: [weese2@llnl.gov](mailto:weese2@llnl.gov)

Phone: (925) 424-3165

Fax: (925) 424-3281



LLM-105

**Abstract**

With the use of modern tools such as molecular modeling on increasingly powerful computers, new materials can be evaluated by their structural activity relationships, SAR, and their approximate physical and chemical properties can be calculated in some cases with surprising accuracy. These new capabilities enable streamlined synthetic routes based on safety, performance and processing requirements, to name a few [1]. Current work includes both understanding properties of old explosives and measuring properties of new ones. The necessity to know and understand the properties of energetic materials is driven by the need to improve performance and enhance stability to various stimuli, such as thermal, friction and impact insult. This review will concentrate on the physical properties of RX-55-AE-5, which is formulated from heterocyclic explosive, 2,6-diamino-3,5-dinitropyrazine-1-oxide, LLM-105, and 2.5 % Viton A. Differential scanning calorimetry, DSC, was used to measure a specific heat capacity,  $C_p$ , of  $\approx 0.950$  J/g $\cdot$  $^{\circ}$ C, and a thermal conductivity,  $\kappa$ , of  $\approx 0.160$  W/m $\cdot$  $^{\circ}$ C. The Lawrence Livermore National Laboratory

(LLNL) code *Kinetics05* and the Advanced Kinetics and Technology Solutions (AKTS) code *Thermokinetics* were both used to calculate Arrhenius kinetics for decomposition of LLM-105. Both obtained an activation energy barrier  $E \approx 180 \text{ kJ mol}^{-1}$  for mass loss in an open pan. Thermal mechanical analysis, TMA, was used to measure the coefficient of thermal expansion, *CTE*. The *CTE* for this formulation was calculated to be  $\approx 61 \text{ }\mu\text{m/m}\cdot^\circ\text{C}$ . Impact, spark, friction and evolved gases are also reported.

Keywords: energetic materials, insensitive explosives, thermal decomposition kinetics, specific heat capacity, thermal conductivity, coefficient of thermal expansion

---

\* To whom correspondence should be addressed. E-mail: weese2@llnl.gov

## 1. Introduction

A new, less sensitive explosive, RX-55AE-5, has been prepared and subjected to physical characterization tests. RX-55AE-5 is formulated from 97.5% 2,6-diamino-3,5-dinitropyrazine-1-oxide (LLM-105) and 2.5% Viton A. Some of its properties are summarized in Table 1 along with a few for LLM-105. LLM-105 has a density of  $1.913 \text{ g/cm}^3$ , a  $Dh_{50}$  of 90-150 cm, and is insensitive to both spark and friction. It has an onset temperature for decomposition of  $348^\circ\text{C}$  at a linear heating rate of  $10^\circ\text{C/min}$  as measured by Differential Scanning Calorimetry (DSC). It is generally insoluble in common organic solvents. In this work, we measure and report the thermal expansion coefficient, thermal decomposition kinetics, and sensitivity to spark, friction, and impact for the RX-55-AE-5 formulation of LLM-105.

Substantial previous work by Pagoria [2] and associates has attempted to discover new insensitive high explosives (IHE) such as LLM-105 that have higher energy densities than 1,3,5-triamino-2,4,6-trinitrobenzene (TATB). TATB is well noted for its thermal stability (m.p.  $> 370^\circ\text{C}$ ); low insensitivity to external stimuli such as drop hammer, spark, and friction; and its very low solubility in a wide array of solvents. We compare our results for RX-55-AE-5 to PBX-9502, LX-17 and TATB [3]. PBX 9502 is formulated from 95% TATB and 5% Kel-F 800 and LX-17 is formulated from 92.5% TATB and 7.5% Kel-F 800.

Table 1: Properties of RX-55-AE [1, 2, 4]

Molecular weight, LLM-105	216.04 g/mol
Color	Yellow
Crystal structure, LLM-105	monoclinic
Crystal density, LLM-105	1.913 g/cm <sup>3</sup>
Coefficient of thermal expansion, CTE	60μm/m•°C
Heat capacity	0.931 J/g/°C
Electrostatic sensitivity	Insensitive

## 2. Experimental

### 2.1 RX-55-AE-5 sample preparation

We used RX-55-AE-5 sample material (LLNL lot PR#1640) for this work; the designation RX-55-AE-5 refers to a research explosive synthesized and processed at LLNL. Pellets of each explosive were uniaxially-pressed in a conventional compaction die without mold release, using a two pressing cycles of 5 minutes at 200 MPa for the larger pellets. The RX-55-AE-5 pellets were pressed at 105°C and obtained densities 1.74 g/cc to 1.75 g/cc (91.0% to 91.5 % theoretical maximum density), TMD) [5]. Pellet properties are summarized in Table 2.

Table 2: RX-55-AE-5 sample mass, volume, density and dimensions

Sample	length, cm	diameter, cm	mass, g	volume, cm <sup>3</sup>	density, g/cm <sup>3</sup>
1	0.643	0.635	0.356	0.204	1.75
2	0.642	.0633	0.356	0.205	1.74

### 2.2 Thermal expansion measurements

We measured the *coefficient of thermal expansion, CTE*, of RX-55-AE-5 using a TA Instruments Model 2940 TMA that was controlled by a TA 500 Thermal Analyzer equipped with a TMA Mechanical Cooling Accessory [6,7]. A quartz micro-expansion probe sat on top of all samples with a force of 0.01 Newtons (N). The change in the length of the sample as it was heated or cooled was measured by a linear transformer that converted the vertical distance of the quartz motion probe and was recorded by the TA Instrument software. Ultra high purity nitrogen carrier gas was used at a constant flow rate of 100 cm<sup>3</sup>/min. Samples were heated at a linear heating rate of 3°C/min.

Temperature, force, probe and cell constant calibrations were carried out as prescribed [7], using NIST standards of indium, lead, tin and zinc metals along with aluminum standard

reference material. *CTE* measurements using a NIST certified aluminum standard had less than  $\pm 2$  % drift associated over the temperature range of  $-20$  to  $100^{\circ}\text{C}$ .

### 2.3 *Decomposition kinetics by thermal analysis* [8]

Weight loss measurements were carried out using a TA Instruments Simultaneous Differential Thermogravimetric Analyzer (SDT), model 2960, manufactured by TA Instruments. The SDT instrument is capable of performing both thermogravimetric analysis (TGA) and differential thermal analysis (DTA) at the same time. We also measured thermal decomposition kinetics and specific heat capacity,  $C_p$ , using differential scanning calorimetry (DSC). DSC analyses of RX-55-AE-5 were carried out using a TA Instruments Model 2920 and TA Instruments pinhole hermetic aluminum pan that had a small perforation in the pan lid to allow generated gases to escape during decomposition. Linear heating rates of 0.1, 0.34, and  $1.0^{\circ}\text{C}$  per minute and a purge gas flow of  $50\text{ cm}^3/\text{min}$  of ultra high purity nitrogen were used for decomposition kinetics. A linear heating rate of  $3^{\circ}\text{C}$  per minute was used for  $C_p$  measurements. Samples sizes were limited to  $<0.5\text{ mg}$  to prevent bursting the pan. Data was analyzed using the LLNL *Kinetics05* program and the AKTS *Thermokinetics* program.

### 2.4 *Friction sensitivity* [9]

The frictional sensitivity of RX-55-AE-5 was evaluated using a B.A.M. high friction sensitivity tester. The tester employs a fixed porcelain pin and a movable porcelain plate that executes a reciprocating motion. Weight affixed to a torsion arm allows for a variation in applied force between 0.5 and 36.0 kg, and our tests used a contact area of  $0.031\text{ cm}^2$ . The relative measure of the frictional sensitivity of a material is based upon the largest pinload at which less than two ignitions (events) occur in ten trials. No reaction is called a “no-go”, while an observed reaction is called a “go.”

### 2.5 *Spark sensitivity* [10]

The sensitivity of RX-55-AE-5 toward electrostatic discharge was measured on a modified Electrical Instrument Services Electrostatic Discharge (ESD) Tester. Samples were loaded into Teflon washers and covered with a 1-mm thick Mylar tape. The density of this packed material was  $1.4\text{ cm}^3/\text{g}$ . The ESD threshold is defined as the highest energy setting at which a reaction occurs for a 1 in 10 series of attempts. Tests were run on powder and pellets at  $68^{\circ}\text{F}$  and a relative humidity of 56%.

### 2.6 *Impact sensitivity (drop hammer)* [11]

An Explosives Research Laboratory Type 12-Drop Weight apparatus, more commonly called a “Drop-Hammer Machine” was used to determine the impact sensitivity of CP

relative to the primary calibration materials PETN, RDX, and Comp B-3 at 68°F and 56% relative humidity. The apparatus was equipped with a Type 12A tool and a 2.5-kg weight. The 35-mg ± 2-mg powder sample was impacted on a Carborundum “fine” (120-grit) flint paper. A “go” was defined as a microphone response of 1.3 V or more as measured by a model 415B Digital Peakmeter. A sample population of 15 was used. The mean height for “go” events, called the “50% Impact Height” or  $Dh_{50}$ , was determined using the Bruceton up-down method.

### 3. Results

#### 3.1 CTE Measurements of RX-55-AE-5

Figure 1 shows two independent TMA analyses and their plots of dimensional change versus temperature over the temperature range of -20°C to 100°C. The plotted dimensional change of the two samples is reproducible. CTE values,  $\alpha$ , were calculated using equation 1

$$\alpha = \frac{dL}{dT * L_o} \tag{1}$$

where  $dL$  is the change in length ( $\mu\text{m}$ ),  $dT$  is the change in temperature ( $^{\circ}\text{C}$ ) and  $L_o$  is the initial sample length (meters). Results are plotted in Figure 2, and average values are listed in Table 3 for six specific temperature intervals.

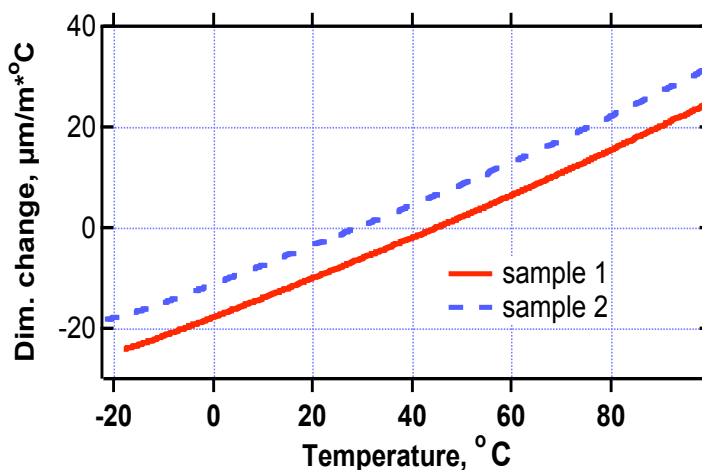


Figure 1: RX-55-AE-5 dimensional change versus temperature.

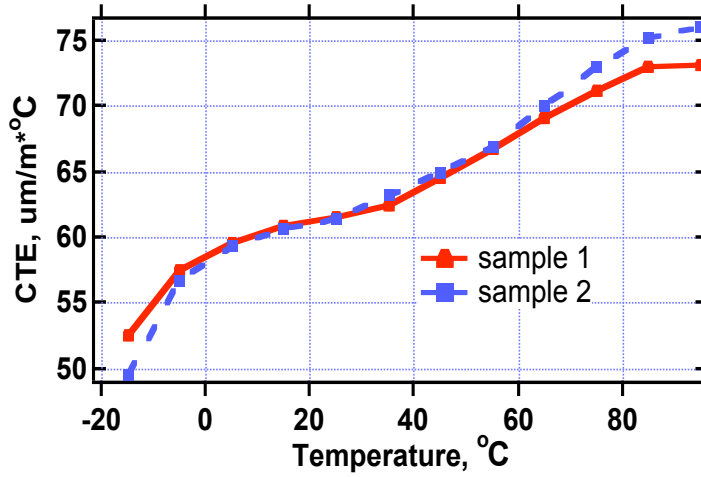


Figure 2: *CTE* versus temperature for RX-55-AE-5 over the temperature range of -20°C to 100°C.

Table 3: RX-55-AE-5 *CTE* values,  $\alpha$ ,  $\mu\text{m}/\text{m}^\circ\text{C}$

Sample	-20°C to 0°C	0°C to 20°C	20°C to 40°C	40°C to 60°C	60°C to 80°C	80°C to 100°C
1	55	60	62	66	70	73
2	56	60	62	66	72	76

### 3.2 Decomposition kinetics

The basic starting equation gives the rate of reaction in terms of a rate constant times a function of the extent of reaction [12, 13]:

$$\frac{d\alpha}{dt} = k(T)f(\alpha) \quad (2)$$

where  $f(\alpha)$  describes the conversion dependence of the rate and the temperature dependence of  $k$  is typically described by an Arrhenius law ( $k=A\exp(-E/RT)$ ), where  $A$  is a frequency factor,  $E$  is an activation energy, and  $R$  is the gas constant.

The simplest methods of kinetic analysis used in *Kinetics05* is Kissinger's method [12], in which the shift of temperature of maximum reaction rate ( $T_{max}$ ) with heating rate ( $\beta$ ) is given by

$$\ln(\beta/T_{max}^2) = -E/RT_{max} + \ln(AR/E). \quad (3)$$

Friedman's isoconversional method [14] involves an Arrhenius analysis at constant levels of conversion, and we determined the apparent first-order frequency factor and activation energy at 1% intervals using both LLNL and AKTS kinetics analysis programs.

Model fitting used the extended Prout-Tompkins model,

$$f(\alpha) = (1-q(1-\alpha))^m(1-\alpha)^n, \quad (1)$$

where  $\alpha$  is the fraction reacted,  $n$  is the reaction order,  $m$  is a nucleation-growth parameter, and  $q$  is an initiation parameter set equal to 0.99. When  $m$  is zero, this model reduces to an  $n$ th-order reaction.

For the SDT data, we considered only mass loss for kinetic analysis. Instability of the DTA baseline meant that results were inconclusive as to whether the mass loss corresponds to an endothermic or exothermic reaction or some combination thereof. Kissinger's method yielded  $A = 2.19 \times 10^{13} \text{ s}^{-1}$  and  $E = 173.5 \text{ kJ/mol}$ , with a standard error of 8.7 kJ/mol on the activation energy. The Friedman parameters are shown in Figure 3 and are approximately equal to the Kissinger value. The AKTS code with its baseline optimization feature has less noise at low conversion, but the two programs agree very well overall.

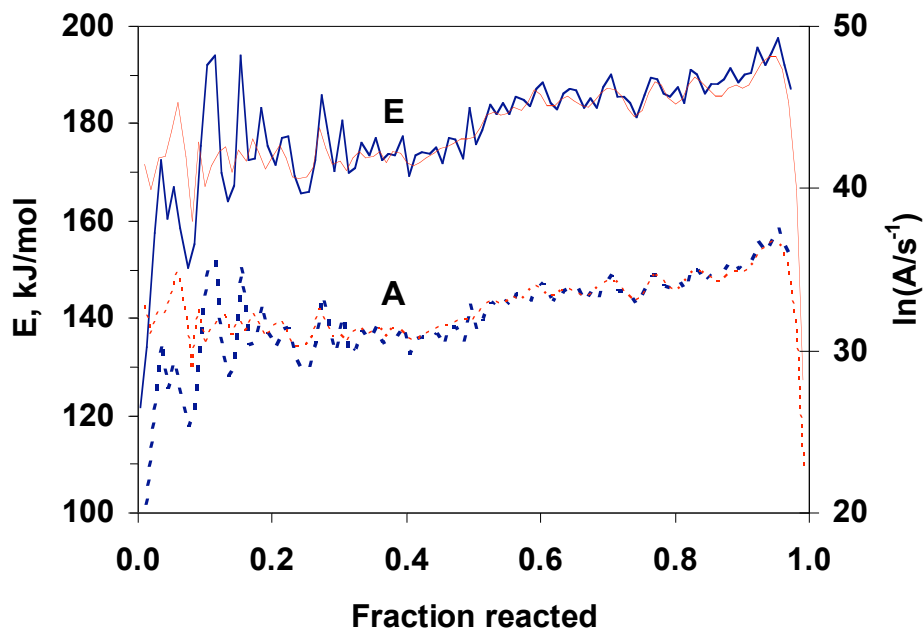


Figure 3: Conversion dependence of  $A$  (dotted line) and  $E$  (solid line) determined by Friedman's method. The bold lines used *Kinetics05* and the thin lines used *Thermokinetics*.

For the model fitting approach, the shape of the reaction profile—the sharp decline past the maximum reaction rate and the direct approach to baseline—suggests an  $n$ th-order reaction with  $n < 1$ . Simultaneously fitting the three cumulative reaction profiles to such a model gave reaction parameters of  $A = 6.20 \times 10^{13} \text{ s}^{-1}$ ,  $E = 172.9 \text{ kJ/mol}$ , and  $n = 0.65$ . A comparison of the measured fractions reacted with those calculated from both the isoconversional and  $n$ th-order fits is shown in Figure 3. The reaction profile is not an ideal  $n$ th-order reaction, so the  $n$ th-order fit shows significant deviation.

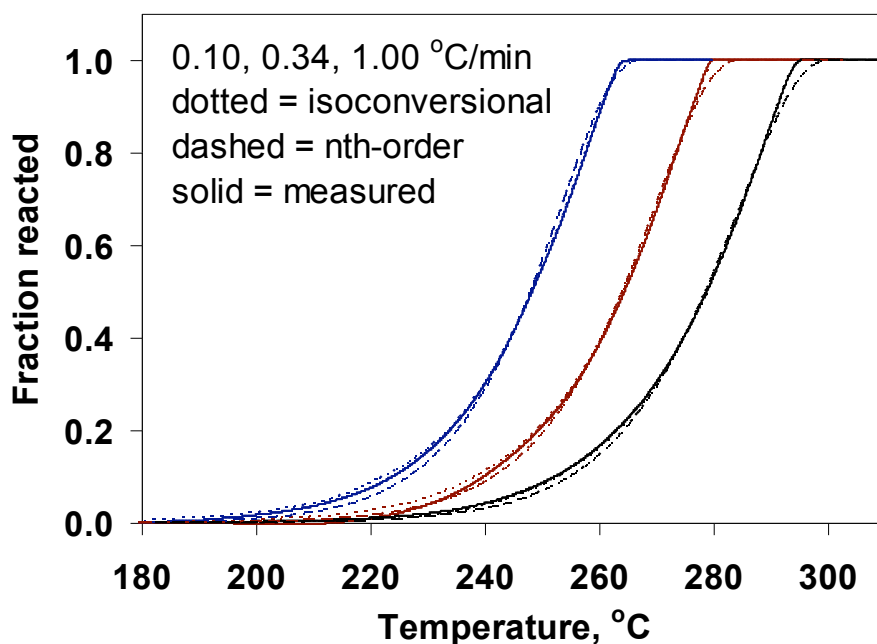


Figure 4: Comparison of integrated experimental data with that calculated from the isoconversional and  $n$ th-order fits.

A better fit can be obtained to the latter stages of reaction by fitting the reaction rates instead of the cumulative reacted, but the fit to the early portion of the reaction is worse. Consequently,  $m$  was also optimized against reaction rates, and the results are shown in Figure 5. The measured and calculated fraction reacted curves are essentially superimposable. The negative nucleation-growth parameter has no physical meaning; it merely serves as a method of fitting the profile shape and width simultaneously.

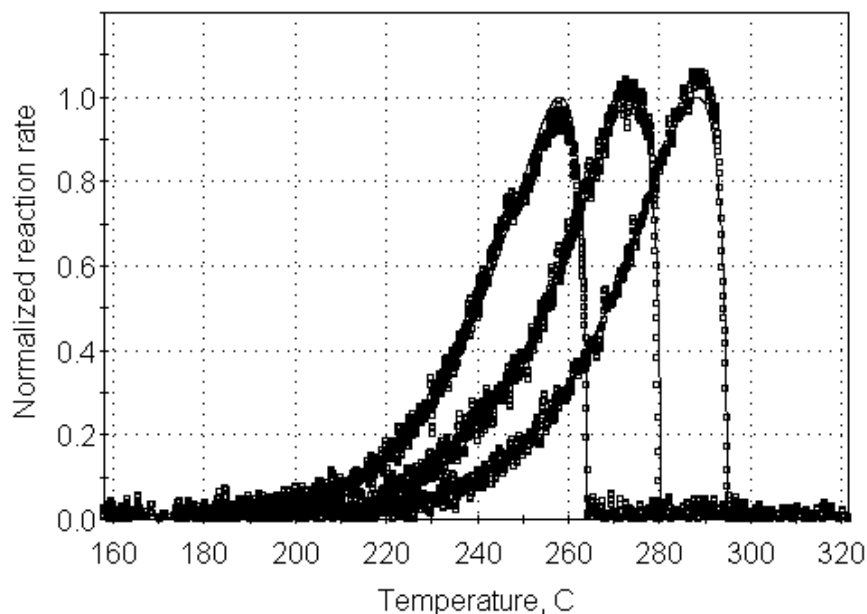


Figure 5. Comparison of measured reaction rates with those calculated from a fit to an extended Prout-Tompkins model, with  $A = 9.06 \times 10^{13} \text{ s}^{-1}$ ,  $E = 182.8 \text{ kJ/mol}$ ,  $n = 0.315$ , and  $m = -0.32$ .

The DSC experiments had variability in peak shape, possibly due to confinement conditions of the sample. Two runs at 0.1 and 1.0 °C/min were selected as most representative of pinhole hermetic pan conditions and analyzed using the Kissinger and Friedman methods. Kissinger's method gave  $A = 8.65 \times 10^{17} \text{ s}^{-1}$  and  $E = 244.3 \text{ kJ/mol}$ . The Friedman parameters are shown in Figure 6 and a comparison of measured and calculated reaction rates is given in Figure 7. The activation energy varies generally between 200 and 250 kJ/mol, and the value near mid conversion agrees with Kissinger's method. The difference in sharpness of the reaction profiles at the two heating rate causes oscillations in the activation energy near 90% conversion. This also causes some instability in the calculated rates at temperatures above the peak reaction rate, but the results are still generally quite good. A model fitting approach would need at least two reactions.

Comparison of the reaction rates in Figures 5 and 7 indicated that the heat release in a sealed pan occurs at ~50 °C higher than mass loss in an open pan, suggesting that sublimation reactions are reduced and secondary reactions are enhanced. This is also

reflected in a  $\sim 50$  kJ/mol increase in the activation energy deduced from a comparison of Figures 4 and 6.

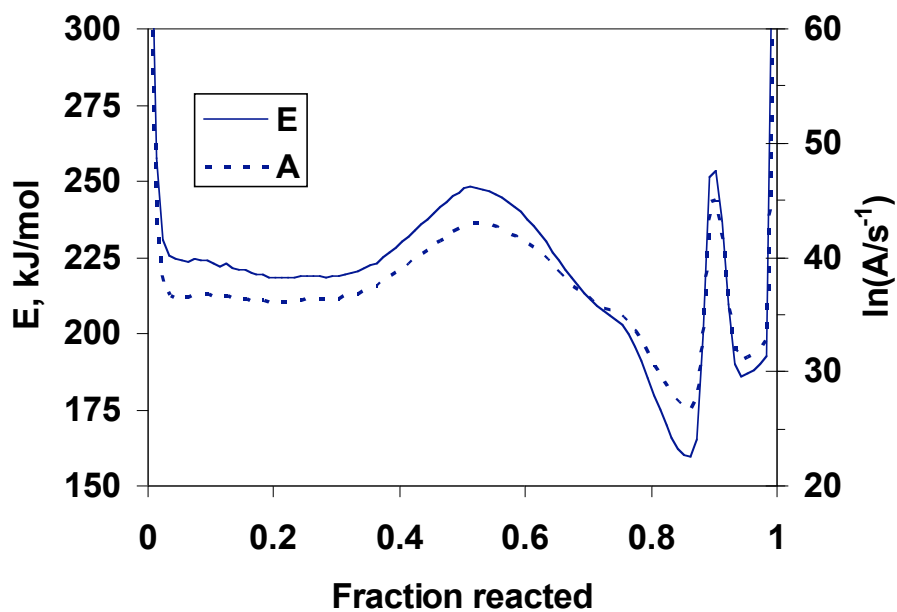


Figure 6. Friedman isoconversional kinetic parameters for DSC heat release from RX-55-AE-5 heated at 0.1 and 1.0 °C/min in a pinhole hermetic pan.

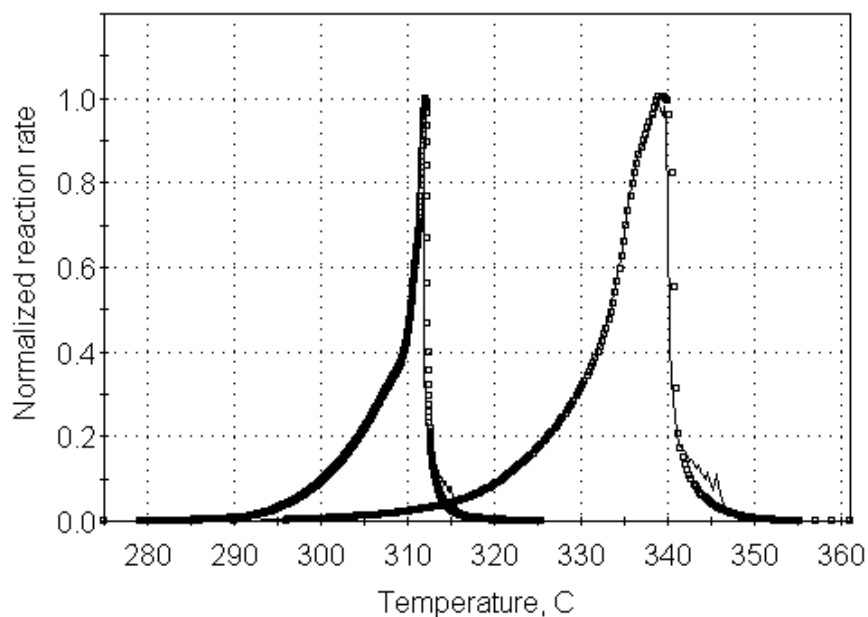


Figure 7. Comparison of measured and calculated reaction rates of RX-55-AE-5 using Friedman's method.

### *Reaction to various stimuli*

Small scale testing (SST) of energetic materials and other compounds is done to determine sensitivity to various stimuli, including friction, impact and static spark. These tests establish parameters for the safety in handling and carrying out experiments that will describe the behavior of materials that are commonly stored for long periods of time. In the friction sensitivity test, RX-55-AE-5 was observed to have 1/10 “goes” at 36.0 kg at 22°C and a relative humidity of 64%. RX-55-AE-5 was compared to an RDX calibration sample, which was also found to have 1 event in 10 trials at 12.4 kg. This material is **not** considered to be friction sensitive. In the spark sensitivity test, no reactions were observed (0/10) at 10 kV (1J). This material is **not** spark sensitive under these specific conditions. In the impact sensitivity test, the  $Dh_{50}$  for RX-55-AE-5 was  $170 \pm 1.0$  cm. For comparison, the  $Dh_{50}$  of PETN, RDX, and Comp B-3 were measured at 15.5, 34.5, and 41.4 cm, respectively.

### **DISCUSSION**

Our various determinations of thermal expansion of RX-55-AE-5 as a function of temperature agree well with each other. However, there are no published data on this new formulation, so we cannot compare to literature results.

We can compare our RX-55-AE-5 results to those for TATB formulations, which our new material is intended to replace. Figure 8 shows expansion data for various lots of PBX 9502 (pressed cold and hot) to give an idea of the spread in CTE values depending on preparation conditions. Table 4 gives the measured mass, length, diameter and calculated densities of the PBX 9502 samples shown in Figure 8. Other parameters, such as particle size, wet aminated or dry aminated, should be considered, but they were not varied in the present work. Maienschein and Garcia [15], who show that variations in CTE values can result from factors such as pressing at elevated temperature versus room temperature. Apparent residual strain is incorporated into the sample from the sample pressing process and is released during heating. Irreversible ratchet growth was observed in LX-17 when thermally cycled and continued to expand when held between 250-285°C for 4-5 hours.

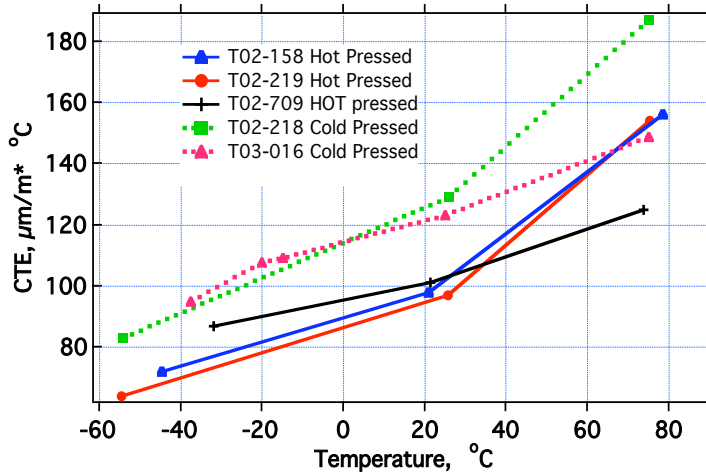


Figure 8: *CTE* values for various lots of PBX 9502 measured in our laboratory.

Table 4: PBX 9502 sample properties.

Material	Sample I.D.	Lot#	Conditions	mass, g	length, cm	diameter, cm	density, g/cm <sup>3</sup>
PBX 9502	T02-158	C-382	Hot pressed	0.374	0.631	0.628	1.91
PBX 9502	T02-219	C-382	Hot Pressed	0.374	0.628	0.631	1.91
PBX 9502	T02-709	C-382	Hot Pressed	0.375	0.630	0.631	1.90
PBX 9502	T02-218	C-382	Cold Pressed	0.375	0.630	0.634	1.88
PBX 9502	T03-016	C-382	Cold Pressed	0.375	0.632	0.634	1.88

Variation in the *CTE* values for PBX 9502 was not the focus of this work; rather it was how the *CTE* values for RX-55-AE-5 would compare to a variety of IHE materials. The comparison of RX-55-AE-5, TATB, LX-17 and PBX 9502 in Table 5 shows that RX-55-AE-5's *CTE* values change the *least* over the temperature range of -25°C to 75°C. Figure 9 makes this comparison graphically. TATB and its formulations have similar slopes that are much greater than that of RX-55-AE-5. While the *CTE* of RX-55-AE-5 is between the two TATB formulations at -25°C, its weaker temperature dependence makes its *CTE* substantially smaller than either LX-17 or PBX 9502 at 75°C.

Table 5: CTE values ( $\mu\text{m}/\text{m}\cdot^\circ\text{C}$ ) for RX-55-AE-5, TATB, LX-17 and PBX 9502.

Temperature, $^\circ\text{C}$	RX-55-AE-5	TATB	LX-17	PBX 9502
-25	56	74	47	64
25	62	105	76	97
75	71	138	107	154

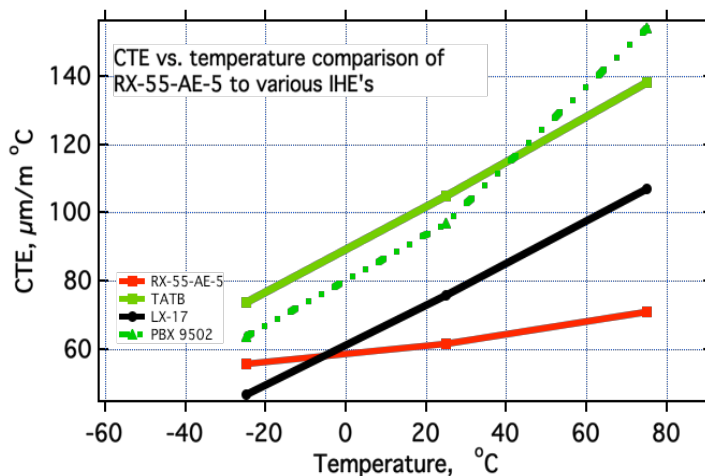


Figure 9: CTE plotted values for RX-55-AE-5, TATB, LX-17 and PBX 9502

Table 6 compares the Small Scale Safety Test (SST) values for RX-55-AE-5, PBX 9502, LX-17, TATB and LLM-105 determined in this work. Thermal decomposition is used to determine the thermal stability of a material with respect to heat [16]. TATB compounds are well known for their stability towards heat and are known to decompose at higher temperatures from 370 to 385 $^\circ\text{C}$ . In Figure 10 we have overlaid thermal decomposition scans of RX-55-AE-5 with PBX 9502 and LX-17 to be compared for thermal stability. RX-55-AE-5 shows a broad decomposition peak. It is not understood why the decomposition peak is so broad and appears to have at least two peaks present. It is clear that the base of the decomposition peak is approximately 10 $^\circ\text{C}$  broader than for PBX 9502 and LX-17. The RX-55-AE-5 sample decomposition temperature appears to be approximately 27 $^\circ\text{C}$  lower than LX-17 and 25 $^\circ\text{C}$  lower than PBX 9502.

RX-55-AE-5, LLM-105, PBX 9502, LX-17 and PBX 9502 were compared. RX-55-AE-5 showed no sensitivity to friction by the method we used in this experiment. The ESD threshold of 1.0 J of energy applied to or RX-55-AE-5 and the other comparison materials showed no reaction for this experiment.  $Dh_{50}$  for RX-55-AE-5 was slightly higher than the pure LLM-105 material and slightly lower than that of PBX 9502, LX-17 and TATB.

Table 6: Summary of Small Scale Safety test results

Test	RX-55-AE-5	LLM-105	PBX 9502	LX-17	TATB
DSC (onset of exotherm, °C)	343	350	383	377	385
Friction (# of goes)	0/10	0/10	0/10	0/10	0/10
ESD threshold (1.0 J)	0/10	0/10	0/10	0/10	0/10
Dh <sub>50</sub> (cm)	170	158	> 177	> 177	> 177
E (kJ/mol)	142	TBD	TBD	TBD	TBD
C <sub>p</sub> , J/g°C	0.950	0.931	1.098	1.125	0.991
κ, W/m°C @ 26.85°C	0.160	TBD	0.552	0.799	0.691
CTE, μm/m°C @ 21°C	61	57	93	60	85

<sup>a</sup>: Samples were approximately 35 mg in mass; no density or sample dimensions are available. #1: LLNL Explosives Handbook. TBD: to be determined later.

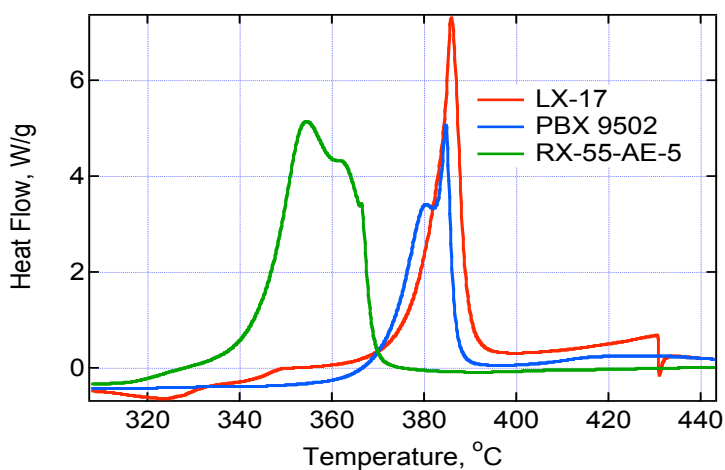


Figure 9: Overlay of DSC decomposition scans for RX-55-AE-5, PBX 9502 and LX-17.

The heat capacity of RX-55-AE-5, PBX 9502 and LX-17 is shown in Figure 10. The heat capacity of RX-55-AE-5 is less than PBX 9502 or LX-17. Heat capacity for LX-17 is slightly higher than PBX 9502.

The thermal conductivity reported here was measured using a TA Instruments 2920 DSC, ran in the modulated mode, thus is commonly referred to as a MDSC [17, 18, 19]. Future work is planned to measure thermal conductivity,  $\kappa$ , for RX-55-AE-5 by means of a pulse laser system.

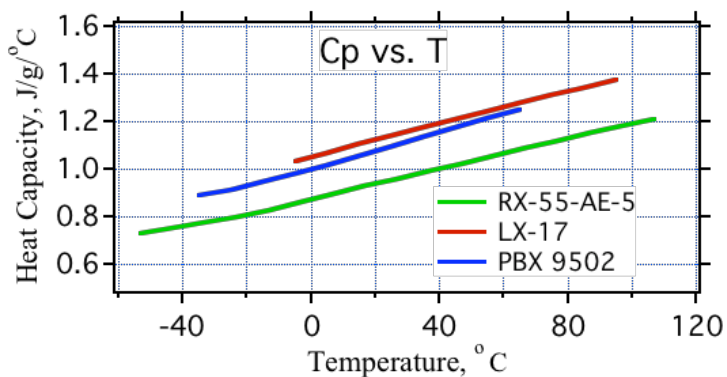


Figure 10: Heat capacity of RX-55-AE-5, PBX 9502 and LX-17 versus temperature.

We have determined that RX-55-AE-5 compares well to PBX 9502 and LX-17. While making this assessment, it became obvious that existing historical data should be compiled in an accessible format, such as the LLNL Explosives Handbook, to facilitate future comparisons.

#### ACKNOWLEDGMENTS

We would like to thank Dr. Craig Tarver and Dr. Phil Pagoria for their technical discussions, help and support on this project. This work performed under the auspices of the U.S. Department of Energy by the University of California, Lawrence Livermore National Laboratory, under Contract number W-7405-Eng-48. UCRL-CONF-212824

## REFERENCES

- [1] T. Tran, R. Simpson, P. Pagoria, M. Hoffman, Written Communication: Updates on LLM-105 development as an insensitive high explosive booster material, JOWOG 9, Lawrence Livermore National Lab, LLNL report UCRL-PRES-145524 (Oct. 2001).
- [2] P. F. Pagoria, G. S. Lee, R. D. Schmidt and A. Mitchell, Synthesis and Scale-Up of 2,6-diamino-3,5-dinitropyrazine-1-oxide (LLM 105) and 2,6-diamino-3,5-dinitropyridine-1-oxide (ANPyO), Submitted to *PEP* (Apr. 2005).
- [3] J. R. Kolb and H. F. Rizzo, Growth of 1,3,5-Triamino-2,4,6-trinitrobenzene, Part I. Anisotropic Thermal Expansion, *PEP* **4**, 10-16 (1979).
- [4] R. D. Gilardi and R. J. Butcher, 2,6-Diamino-3,5-dinitro-1,4-pyrazine 1-oxide, *Acta Cryst.* **E57**, o657-o658 (2001).
- [5] B. M. Dobratz, "LLNL Explosives Handbook-Properties of Chemical Explosives and Explosive Simulants"; LLNL Report UCRL-52997, March 16, 1982; with Errata of Jan. 28, 1982.
- [6] Anonymous, TA Instruments, TA Applications Brief, TA 019, **1998**, New Castle, DE.
- [7] Anonymous, TA Instruments, TMA 2940 Manual, **1996**, TA Instruments, New Castle, DE.
- [8] J. W. Dodd and K. H. Tonge, "Thermal Methods," Jon Wiley and Sons, Crown Copyright, 1987.
- [9] L. R. Simpson and M. F. Foltz, LLNL Small-scale Friction Sensitivity (BAM) Test, LLNL Report UCRL-ID-124563 (Jun. 1996).
- [10] L. R. Simpson and M. F. Foltz, LLNL Small-scale Static Spark Machine: Static Spark Sensitivity Test, LLNL Report UCRL-ID-135525 (Aug. 1999).
- [11] L. R. Simpson and M. F. Foltz, LLNL Small-scale Drop-hammer Impact Sensitivity Test, LLNL Report UCRL-ID-119665 (Jan. 1005).
- [12] H. E. Kissinger, Reaction Kinetics in Differential Thermal Analysis, *Anal. Chem.* **29**, 1702-1706 (1957).
- [13] T. M. Massis, P.K. Morenus, D. H. Huskisson and R. M. Merrill, Stability and Compatability Studies With The Inorganic Explosive CP, *J. of Hazardous Materials* **5**, 309-323 (1982).

- [14] H. L. Friedman, "Kinetics of Thermal Degradation of Char-Forming Plastics from Thermogravimetry. Application to a Phenolic Plastic," *J. Polymer Sci.* **C6**, 183-195 (1964).
- [15] J. L. Maienschein, F. Garcia, Thermal Expansion of TATB-based explosives from 300 to 566 K, *Thermochim. Acta* **384**, 71-83, (2002).
- [16] A. K. Burnham, R. K. Weese and W. J. Andrzejewski, Kinetics of HMX and CP Decomposition and Their Extrapolation for Lifetime Assessment, LLNL Report UCRL-TR-208411 (Dec. 2004); also, these proceedings.
- [17] Modulated DSC Compendium, Basic Theory and Experimental Conditions, TA Applications Brief, TA Instruments, New Castle, Delaware.
- [18] S. M. Marcus and R. L. Blaine, "Thermal conductivity of polymers, glasses and ceramics by modulated DSC," *Thermochim. Acta* **243**, 231-239 (1994).
- [19] R. K. Weese, Thermal conductivity of Tetryl by modulated differential scanning calorimetry, *Thermochim. Acta* **429**, 119-123 (2005).